Proc. Natl. Acad. Sci. USA
Vol. 84, pp. 6162–6166, September 1987
Biophysics

Structure of the reaction center from *Rhodobacter sphaeroides* R-26: The protein subunits*

(bacterial photosynthesis/membrane protein structure/x-ray diffraction/cytochrome *c*–reaction center complex)

J. P. ALLEN†, G. FEHER†‡, T. O. YEATES§, H. KOMIYA§, AND D. C. REES§

†University of California, San Diego, La Jolla, CA 92093; and §University of California, Los Angeles, CA 90024

Contributed by G. Feher, May 18, 1987

ABSTRACT **The three-dimensional structure of the protein subunits of the reaction center (RC) of *Rhodobacter sphaeroides* has been determined by x-ray diffraction at a resolution of 2.8 Å with an *R* factor of 26%. The L and M subunits each contain five transmembrane helices and several helices that do not span the membrane. The L and M subunits are related to each other by a 2-fold rotational symmetry axis that is approximately the same as that determined for the cofactors. The H subunit has one transmembrane helix and a globular domain on the cytoplasmic side, which contains a helix that does not span the membrane and several β-sheets. The structural homology with RCs from other purple bacteria is discussed. A structure of the complex formed between the water soluble cytochrome c_2 and the RC from *Rb. sphaeroides* is proposed.**

The reaction center (RC) from photosynthetic bacteria is an integral membrane protein complex, which contains a number of cofactors that mediate the primary photochemistry. The RC of *Rhodobacter sphaeroides* is composed of three protein subunits L, M, and H having 281, 307, and 260 residues, respectively (1–3). From an analysis of the amino acid sequence of the subunits, five membrane-spanning helices in both the L and M subunits and one in the H subunit were predicted (1–3). Furthermore, labeling experiments showed that the RC spans the membrane with the bulk of the H subunit on the cytoplasmic side; the amino terminus of L was determined to be on the cytoplasmic side (for reviews, see refs. 4 and 5).

The three-dimensional structure of the RC has been obtained to a resolution of 2.8 Å. In a previous paper, we described the x-ray diffraction analysis and reported the structure of the cofactors (6). In this paper, we present the structure of the individual subunits as well as the entire RC complex. A structure of the complex between the RC and the water soluble cytochrome c_2 is proposed. The overall structure and homology with other RCs, in particular that of *Rhodopseudomonas viridis* (7), is discussed.

METHODS

RC crystals having the space group $P2_12_12_1$ were analyzed by x-ray diffraction as described (6). The structure of the RC was determined at a resolution of 2.8 Å with an *R* factor of 26% between calculated and observed structure factors. The secondary structure was identified on the basis of main-chain hydrogen bonding and torsion angle patterns. Due to deviations from ideal geometry, the boundaries of the regions of α-helices and β-sheets have an uncertainty of several residues. Final assignments of the boundaries were checked visually by computer graphics [Evans and Sutherland PS 300 with FRODO program (8)].

The directions of the helical axes were equated with the normals of the greatest square plane fit of the C^α atoms of each helix (9). The radius of curvature to an α-helix was calculated by two methods: (*i*) from the radius of the best circle fit to the projections of C^α atoms onto the helical axis (10); and (*ii*) from the directions of the helical axes based on residues in the first and last halves of a specified helix. If the helix is smoothly distorted into a circle, then these helical directions describe the tangents to a circle that passes through the midpoints of the two sections. From the angle θ between these two directions and the number of residues in the helix, n, the radius of curvature, R, can be estimated (assuming standard helical geometries) from the relationship: $R = 43n/\theta$, where R is in Å and θ is in degrees. The radii of curvature estimated by each method agreed to within 20%, which provides an estimate of the accuracy of the quoted values. Both methods assume that the helix is smoothly distorted into a circle. Since kinking mechanisms undoubtedly contribute to the distortions in these helices, the radii of curvature are useful primarily as an estimate of the extent of bending in each helix.

RESULTS AND DISCUSSION

The Individual Subunits L, M, and H. The structures of the three individual subunits of the RC are shown separately in Fig. 1. Their relative positions have been maintained in the presentation; a superposition of the three frames will, therefore, produce the structure of the RC as discussed later. All residues have been fit to the electron density map except for 6 residues at the carboxyl terminus of L and residues 48–53 of the H subunit.

The most conspicuous feature of the L and M subunits is the presence of the five membrane-spanning helices. Following the nomenclature of Diesenhofer *et al.* (7), they are labeled sequentially A–E (Table 1; Fig. 1). Analysis of the protein sequences (1–3) correctly predicted each helix and most of the residues forming the helices. The outermost helices A and B as well as the D helices are straight. In contrast, the C and E helices are curved, possibly due to steric constraints imposed by the steeply tilted D helices of the opposing subunits and the cofactors.

On the cytoplasmic side, L has one and M has two helices connecting helices D and E; they are labeled de′ and de (see Table 1). In addition, the regions of the amino termini contain the short a-helices and antiparallel β-sheets (regions L24–27, L28–31, M29–34, M43–52) where L and M refer to the L and M subunits, respectively.

The publication costs of this article were defrayed in part by page charge payment. This article must therefore be hereby marked "*advertisement*" in accordance with 18 U.S.C. §1734 solely to indicate this fact.

Abbreviations: RC, reaction center; $Bchl_2$, bacteriochlorophyll dimer; Bchl, bacteriochlorophyll; Q_A and Q_B, primary and secondary quinones, respectively.

*This paper is no. 2 in a series. Paper no. 1 is ref. 6.

‡To whom reprint requests should be addressed.

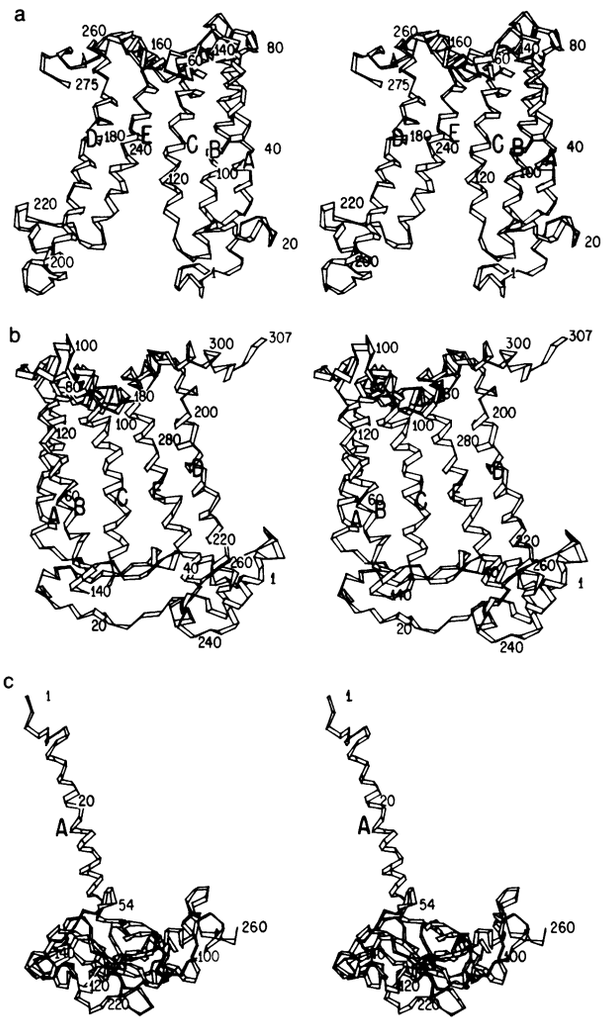

FIG. 1. Stereoviews of the C^{α} backbone of the individual subunits L (*a*), M (*b*), and H (*c*) drawn with the aid of the program of ref. 11. The transmembrane helices are labeled A, B, C, D, and E; selected residues have been numbered. Residues 48–53 of the H subunit have been omitted. The cytoplasmic side is at the bottom of each figure.

On the periplasmic side, the L and M subunits have an interrupted helix, labeled I (see Table 1). The I helix consists of three helical segments connecting helices A and B, C and D, and one following helix E; they are labeled ab, cd, and e, respectively. The three segments are approximately aligned with their helical axes colinear. The I helices are the only amphipathic helices of the RC. On the periplasmic side are also two segments containing β-strands. One connects ab to the B helix (L65–L82; M90–M108); the other connects the C helix to cd (L139–L148; M169–M177).

The secondary structure of the H subunit is very different from that of the L or M subunits. The H subunit has only one transmembrane helix, A, that starts on the periplasmic side near the amino terminus. The bulk of H lies on the cytoplasmic side. Residues 40–102 form an irregular region with an antiparallel β-sheet (58–68 and 69–75). The remaining residues form a globular domain with one nonmembrane spanning helix, a, and two regions of β-sheets (158–170, 174–184; 186–192, and 151–156, 194–200, 201–206). The lack of observed electron density for residues 48–53 is apparently due to disorder of this region in the crystals. A similar situation was encountered in *R. viridis* for residues 48–56 (7).

The LM Complex. The LM complex is capable of performing the charge separation between the bacteriochlorophyll dimer ($Bchl_2$) and the primary quinone (Q_A) (12). The main effect of removing the H subunit is a change in the properties of the quinones (13) (e.g., Q_A can accept two electrons; furthermore, electron transfer to the secondary quinone, Q_B, is inhibited).

Table 1. Characterization of the helices of the reaction center from *Rb. sphaeroides*

Subunit	Helix	Residues (*n*)	Angle between helix and 2-fold axis*	Radius of curvature,† Å
		Membrane-spanning helices		
L	A	32– 55 (24)	25°	>100
	B	83–111 (29)	10°	>100
	C	116–138 (23)	15°	30
	D	171–198 (28)	35°	>100
	E	225–250 (26)	20°	70
M	A	54– 78 (25)	25°	>100
	B	109–139 (31)	15°	>100
	C	147–168 (22)	20°	30
	D	200–226 (27)	35°	90
	E	262–286 (25)	25°	50
H	A	12– 37 (26)	20°	90
		Non-membrane-spanning helices		
L	a	3– 10 (8)	90°	
	I ab	59– 64 (6)		
	I cd	149–165 (17)	85°	
	I e	258–268 (11)		
	de	208–221 (14)	35°	
M	a	35– 42 (8)	80°	
	I ab	81– 89 (9)		
	I cd	178–194 (17)	80°	
	I e	293–302 (10)		
	de′	233–240 (8)	65°	
	de	242–257 (16)	35°	
H	a	227–244 (18)	65°	

n, Number of residues.
*Estimated error, approximately ±5°.
†Estimated accuracy, ±20% (see *Methods*).

The LM complex has a 2-fold rotational symmetry axis that approximately relates the two subunits. We determined the transformation matrix that relates equivalent C^{α} of the membrane spanning helices of the two subunits by the same procedure that was used for the symmetry relation of the cofactors (6). The transformation with the lowest rms deviation (1.2 Å) between equivalent atoms results in a rotation axis given by the polar angles $\phi = 81°$, $\Psi = 53°$, and $\kappa = 180°$. When all cofactors were considered, a slight deviation from this axis was found ($\phi = 81°$, $\Psi = 52°$, $\kappa = 183°$). Since this deviation is so small, we shall consider the symmetry axes of the cofactors and the LM subunits as equivalent in all subsequent discussions.

The LM complex has a core region formed by the D and E helices of each subunit (Fig. 2). The helices of the two subunits cross each other, causing extensive contacts between the two subunits. Each of the D and E helices contain a histidine; they form four nitrogen ligands to the Fe^{2+} (6). This suggests that a possible role of Fe^{2+} is to stabilize the core region. In addition to the transmembrane helices, each subunit has a helix (de) that enters but does not span the membrane. These helices form pockets around Q_A and Q_B. The M subunit has an additional small helix (de′) that passes approximately through the 2-fold axis. It contains Glu-M232, which forms the remaining two ligands with Fe^{2+}.

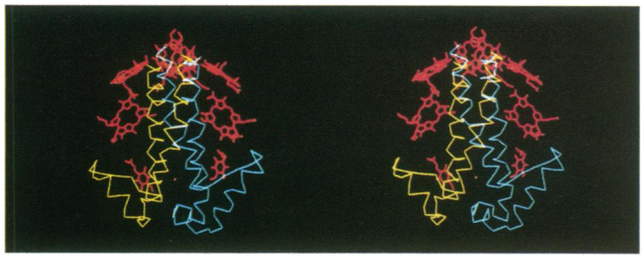

FIG. 2. Stereoviews of the "core" (D and E helices) of the LM complex with the L subunit (yellow), M subunit (blue), and pigments (red). For clarity, the phytyl and isoprenoid chains have been truncated. The 2-fold axis runs vertically in the plane of the figure. The cytoplasmic side is at the bottom of the figure.

The outer region of the LM complex is formed by the membrane spanning helices A, B, and C; the I helices; and the regions of the amino termini. On the periplasmic side, the I helices cross the width of the RC; their axes lie approximately perpendicular to the 2-fold axis and parallel to the normals of the planes of $Bchl_2$. The cytoplasmic side is formed by the residues near the amino termini, which span the region between the A and D helices. The outer region can be visualized as a "cage" enclosing the core and the cofactors (Fig. 3).

The Overall Structure of the RC. The overall structure of the RC is shown in Figs. 4 and 5. As mentioned earlier, the most striking feature is the presence of 11 transmembrane helices consisting of 22–31 residues (Table 1). The helices are not all parallel to each other; for example, the angle between the D helices of the L and M subunits is 65°. The transmembrane helix of the H subunit runs approximately antiparallel to the E helix of the M subunit and makes several contacts with it. In addition, there are several non-membrane-spanning helices and several β-sheets. The total α-helical content of the RC is 51% (Table 1), which is in agreement with the value of 50% ± 10% obtained from circular dichroism studies (14). The globular domain of the H subunit makes many contacts with the cytoplasmic side of the L and M subunits.

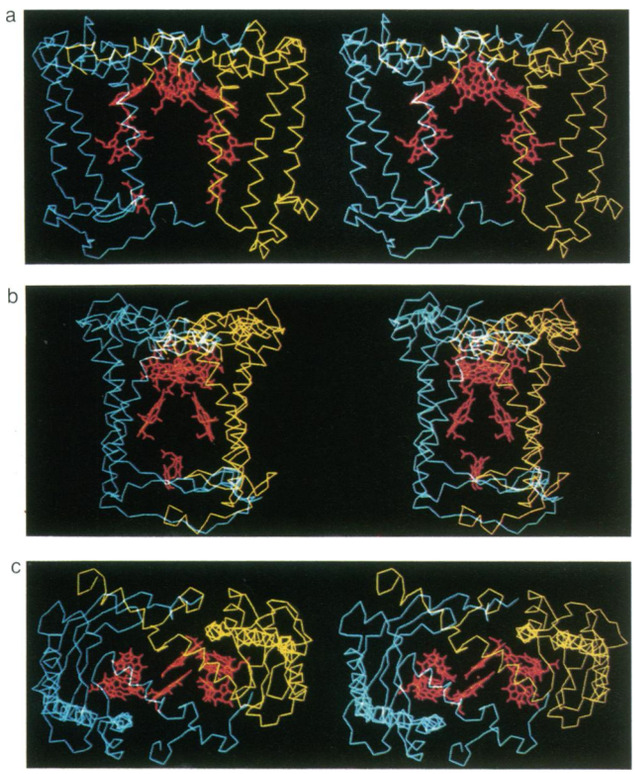

FIG. 3. Stereoviews of the outer region (amino terminus to C-helix) of the LM complex with the L subunit (yellow), M subunit (blue), and pigments (red). Phytyl and isoprenoid chains of the cofactors have been truncated. (*a*) RC in the same orientation as in Fig. 2. (*b*) Related to *a* by a rotation of ≈90° around the 2-fold axis. (*c*) View down the 2-fold axis; note the special pair and Fe^{2+} in the center.

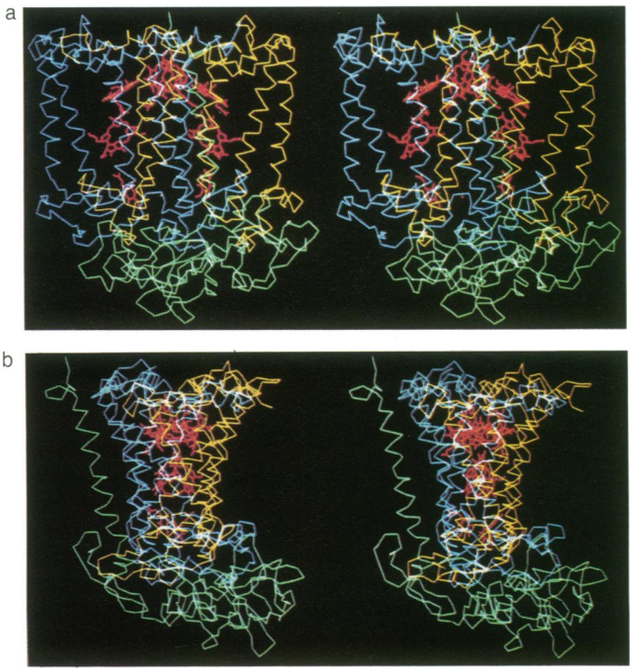

FIG. 4. Stereoview of the RC structure with the L (yellow), M (blue), and H (green) subunits, and the cofactors (red) with truncated phytyl and isoprenoid chains. Electron transfer proceeds preferentially along the chain of cofactors on the right side, which is called the A branch (6). (*a*) RC in the same orientation as in Figs. 2 and 3*a*. (*b*) Related to *a* by a rotation of ≈90° around the 2-fold axis. The cytoplasmic side is at the bottom of each figure.

The structure suggests several possible roles for the H subunit. The transmembrane helix is closer to the A branch of the cofactors (6) and may contribute to the preferential electron transfer along that branch.¶ The extensive contacts of H with LM may stabilize the RC structure. When H is removed, the quinones are dramatically affected (13). This may be due to a loosening of the LM structure, which makes the Q_A site accessible to solvent and allows Q_A to accept two electrons. Similarly, the loosened structure may have a lower binding constant for Q_B, accounting for the impaired electron transfer from Q_A^- to Q_B.

The distribution of hydrophilic and hydrophobic residues of the RC is consistent with it being an integral membrane protein. There are no charged residues in the middle region of the RC (see Fig. 6). Consequently, we associate this part of the RC with the interior of the membrane region. Consistent with this is the presence of the long α-helices that meet hydrogen bonding requirements of the backbone atoms internally. A more detailed account of the energetics of this situation will be presented in a forthcoming paper (15).

The RC–Cytochrome Complex. In *Rb. sphaeroides*, the primary donor $Bchl_2$ is reduced by a water-soluble cytochrome c_2. The RC has one cytochrome c_2 binding site (16)

¶The influence of the H subunit on the cofactors is demonstrated by the elimination of the splitting of the low-temperature optical absorption at 537 nm of the bacteriopheophytin when the H subunit is removed (13).

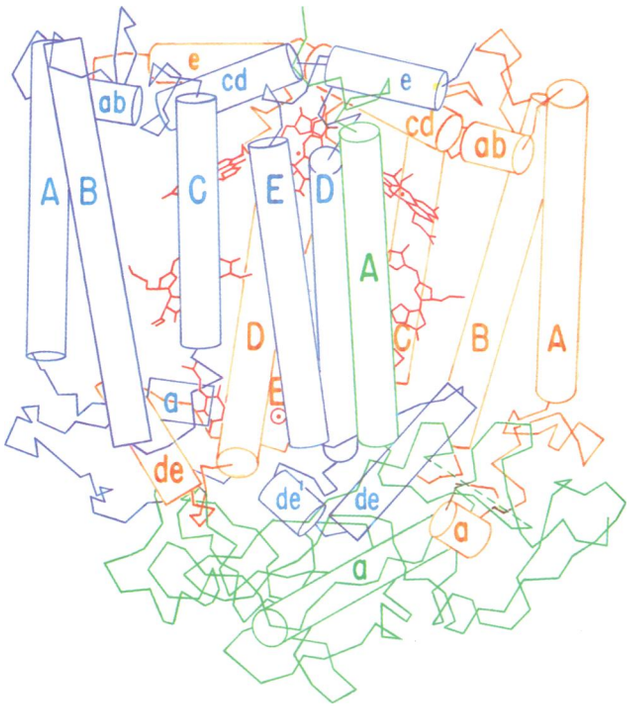

FIG. 5. The RC structure with L (yellow), M (blue), and H (green) subunits and the cofactors (red) with truncated phytyl and isoprenoid chains. The α-helices have been approximated by straight cylinders (Table 1 lists their curvatures). The view is the same as that shown in Fig. 4*a*. The dotted line in the C^{α} backbone of H corresponds to residues 48–53, for which only a weak electron density was obtained. The circle (red) near the bottom of the D and E helices is the position of the nonheme iron.

on the periplasmic side of the membrane (17), which is shared by both the L and M subunits (18). The binding domain on the RC contains negatively charged carboxylate groups (19) that are believed to interact electrostatically (for a review, see ref. 20), with lysine residues surrounding the heme crevice of cytochrome c_2 (21).

There is a strong homology among cytochromes from different species (22, 23). Many key residues are conserved and the different cytochromes exhibit similar folding patterns. Different cytochromes (e.g., cytochrome c_2 from *Rb. sphaeroides* or *Rhodospirillum rubrum*, horse heart cytochrome *c*) can reduce $Bchl_2^+$ from *Rb. sphaeroides*, albeit with different rate constants. The only cytochrome c_2 from purple bacteria whose three-dimensional structure has been determined is that from *Rs. rubrum* (24).

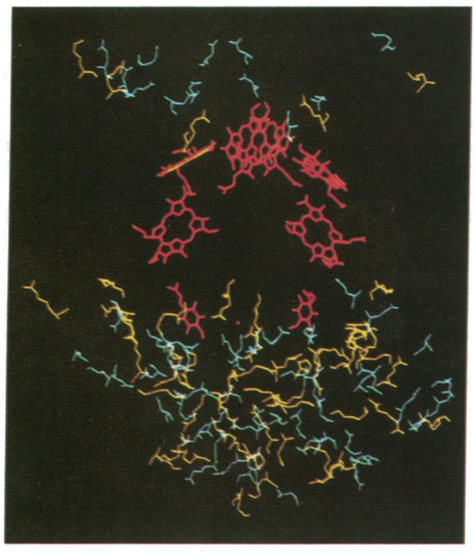

FIG. 6. The charged residues Glu and Asp (blue), Lys and Arg (yellow), and the truncated cofactors (red) of the RC. The view is the same as shown in Fig. 4*a*. Note the absence of charged residues in the central region of the membrane.

The following procedure was adopted to obtain the structure of the RC–cytochrome c_2 complex. The cytochrome c_2 from *R. rubrum* was initially positioned relative to the RC to form the following salt bridges: Lys-C27 to Asp-L155, Lys-C90 to Asp-L257, and Lys-C94 to Asp-M184, where L, M, and C denote the L and M subunits and cytochrome c_2, respectively. These residues of the heme crevice region of cytochrome were chosen since they are conserved between species and because the resulting structure produced a parallel orientation of the cytochrome heme with the $Bchl_2$ of the RC, which is believed to optimize electron transfer (25). The structure was then adjusted manually to exclude interpenetrating van der Waals spheres, between the cytochrome and RC by moving the cytochrome as a rigid body using the FRODO program (8). The resulting structure changed the configuration of some of the original salt bridges. It should be noted that the proposed structure has not been determined to be unique.

The resulting structure of the RC–cytochrome complex is shown in Fig. 7. The planes of the heme and the $Bchl_2$ are approximately parallel. The distance between the heme Fe and the Mgs of either Bchl of the dimer is 19 Å; the distance of closest approach between the heme ring and the $Bchl_2$ tetrapyrrole rings is 11 Å. The distance from the heme iron to the Fe^{2+} of the RC is 45 Å, in agreement with the values measured by x-ray resonance experiments (26). Midway between the heme and $Bchl_2$ is the residue Tyr-L162. The aromatic ring of Tyr-L162 is 4 Å from the heme ring and 6 Å from the tetrapyrrole rings of $Bchl_2$. The angle between the normals of the tyrosine ring and the heme is approximately 50° and between the tyrosine and the tetrapyrrole rings of the dimer is 60°.

The residues involved in the binding of cytochrome c_2 to the RC are shown in Fig. 8. Salt bridges can be formed between C12 and M292, C27 and L155, C88 and L257, C97 and M95, with possible additional salt bridges between C9, C13, C75, C90, C94 and L72, L261, M100, M173, M184. All the RC residues listed, except M173, are conserved between *Rb. sphaeroides* and *Rhodopseudomonas capsulata*. The assignment of salt bridges is limited by the lack of knowledge concerning conformational changes that may occur when the cytochrome c_2 approaches the RC. The involvement of

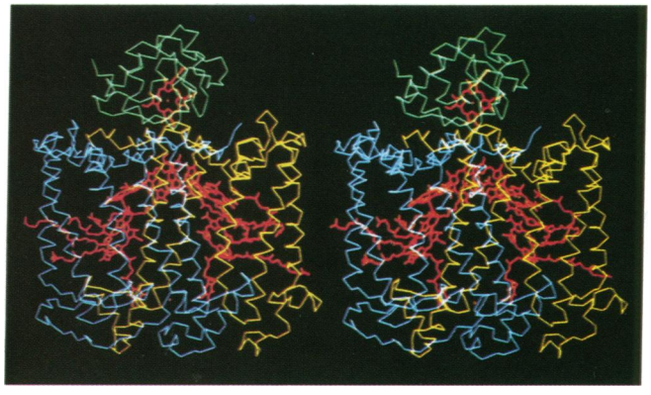

FIG. 7. Stereoview of a model cytochrome c_2 with its heme (red) docked to the LM complex [L (yellow), M (blue)] with the cofactors (including the phytyl and isoprenoid chains) in red. The 2-fold axis is in the plane of the figure. The cytoplasmic side is at the bottom of the figure.

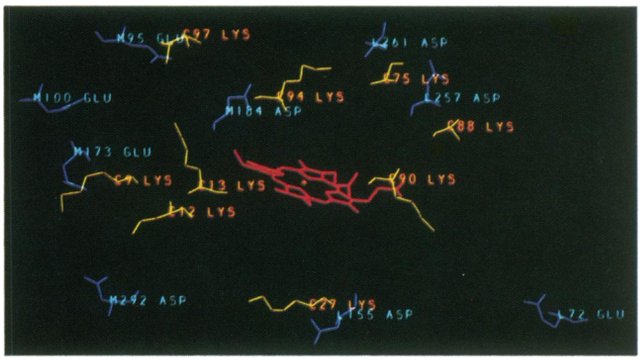

FIG. 8. The Asp and Glu residues of the RC (blue) and the Lys of cytochrome c_2 (yellow) that are proposed to be involved in the binding of the cytochrome c_2 (heme in red). The RC–cytochrome c_2 complex is oriented with the 2-fold axis normal to the plane of the paper.

lysines from the heme crevice region in the binding of cytochrome to the RC is consistent with the experimental results of Hall *et al.* (21). The possibility of an intermediate binding site involving the residues on the back of the cytochrome has been postulated recently (27).

Comparison of RC Structures from Different Bacterial Species. The structure of the RC from *Rb. sphaeroides* is very similar to the one described for *R. viridis* (7). One difference between the two structures is the presence in *R. viridis* of a fourth tightly bound subunit, a cytochrome with four *c*-type hemes. The region of the carboxyl terminus of M has 18 more residues in *R. viridis* than in *Rb. sphaeroides*. These additional residues may be responsible for the formation of the more tightly bound RC–cytochrome complex in *R. viridis* (7).

The distance of the heme closest to the $BChl_2$ in *R. viridis* is positioned similarly to the heme in the model of the RC–cytochrome complex of *Rb. sphaeroides*—i.e., in *R. viridis* the distance of the Fe^{2+} to the Mgs of the $BChl_2$ is 20.5 Å. The average angle between the normals of the tetrapyrrole rings and the heme is ≈40° (compared to 19 Å and 10° in *Rb. sphaeroides*).

The similarity between the three-dimensional structures of the RCs of *Rb. sphaeroides* and *R. viridis* is consistent with the similarity of their primary structures. The protein sequences of the RC have been determined for three species, *Rb. sphaeroides* (1–3), *R. capsulata* (28), and *R. viridis* (29, 30). The percentage identity of the residues conserved in all three species is 53% for L, 46% for M, and 31% for H. Residues that interact with the cofactors tend to be conserved (e.g., the histidines that bind to the Mgs of the Bchls). In addition, the following regions of the RC are well conserved in all three species. The region of the amino terminus of L (25 of 30), the B helix of L (22 of 29), and the region from the middle of the D helix to the E helix of M (45 of 55). All three of these regions surround the cofactors of the A branch. Although the H subunit is poorly conserved overall, the regions of H in contact with the conserved regions of L and M are highly conserved [e.g., residues H30–H42 (69%) and H229–H240 (66%)].

We thank E. Abresch for the preparation of the RCs. This work was supported by grants from the National Institutes of Health (AM36053, GM13191, GM31299, and GM07185), the National Science Foundation (DMB85-18922), a Presidential Young Investigators Award, and the Chicago Community Trust/Searle Scholars Program.

1. Williams, J. C., Steiner, L. A., Ogden, R. C., Simon, M. I. & Feher, G. (1983) *Proc. Natl. Acad. Sci. USA* **80,** 6505–6509.
2. Williams, J. C., Steiner, L. A., Feher, G. & Simon, M. I. (1984) *Proc. Natl. Acad. Sci. USA* **81,** 7303–7307.
3. Williams, J. C., Steiner, L. A. & Feher, G. (1986) *Proteins* **1,** 312–325.
4. Valkirs, G. & Feher, G. (1982) *J. Cell Biol.* **95,** 179–188.
5. Bachofen, R. & Wiemken (1986) *Photosynthesis III* (Springer, New York), pp. 620–631.
6. Allen, J. P., Feher, G., Yeates, T. O., Komiya, H. & Rees, D. C. (1987) *Proc. Natl. Acad. Sci. USA* **84,** 5730–5734.
7. Deisenhofer, J., Epp, O., Miki, K., Huber, R. & Michel, H. (1985) *Nature (London)* **318,** 618–624.
8. Jones, T. A. (1985) *Methods Enzymol.* **115,** 157–171.
9. Schomaker, V., Waser, J., Marsh, R. E. & Bergman, G. (1959) *Acta Crystallogr.* **12,** 600–604.
10. Blundell, T., Barlow, D., Borkakoti, N. & Thornton, J. (1983) *Nature (London)* **306,** 281–283.
11. Lesk, A. M. & Hardman, K. D. (1982) *Science* **216,** 539–540.
12. Feher, G. & Okamura, M. Y. (1978) in *The Photosynthetic Bacteria*, eds. Clayton, R. K. & Sistrom, W. R. (Plenum, New York), pp. 349–386.
13. Debus, R. J., Feher, G. & Okamura, M. Y. (1985) *Biochemistry* **2,** 2488–2500.
14. Nabedryk, E., Tiede, D. M., Dutton, P. L. & Breton, J. (1982) *Biochim. Biophys. Acta* **682,** 273–280.
15. Yeates, T. O., Komiya, H., Rees, D. C., Feher, G. & Allen, J. P. (1987) *Proc. Natl. Acad. Sci. USA* **84,** in press.
16. Rosen, D., Okamura, M. Y., Abresch, E. C., Valkirs, G. E. & Feher, G. (1983) *Biochemistry* **22,** 335–341.
17. Prince, R. C., Baccarini-Melandri, A., Hauska, G. A., Melandri, B. A. & Crofts, A. R. (1975) *Biochim. Biophys. Acta* **387,** 212–227.
18. Rosen, D., Okamura, M. Y., Abresch, E. C., Valkirs, G. E. & Feher, G. (1983) *Biochemistry* **22,** 335–341.
19. Okamura, M. Y. & Feher, G. (1983) *Biophys. J.* **41,** 122a (abstr.).
20. Margoliash, E. & Bosshard, H. R. (1983) *Trends Biochem. Sci.* **8,** 316–320.
21. Hall, J., Zha, X., Durham, B., O'Brien, P., Vieira, B., Davis, D., Okamura, M. & Millett, F. (1987) *Biochemistry* **26,** 4494–4500.
22. Dickerson, R. E. (1980) *Sci. Am.* **242,** 136–153.
23. Meyer, T. E. & Kamen, M. D. (1982) *Adv. Protein Chem.* **35,** 105–212.
24. Salemme, F. R., Freer, S. T., Xuong, N. H., Alden, R. A. & Kraut, J. (1973) *J. Biol. Chem.* **248,** 3910–3921.
25. Salemme, F. R. (1976) *J. Mol. Biol.* **102,** 563–568.
26. Blasie, J. K., Pachence, J. M., Tavormina, A., Dutton, P. L., Stamatoff, J., Eisenberger, P. & Brown, G. (1983) *Biochim. Biophys. Acta* **723,** 350–357.
27. Bosshard, H. R., Snozzi, M. & Bachofen, R. (1987) *J. Bioenerg. Biomembr.* **19,** 375–382.
28. Youvan, D. C., Bylina, E. J., Alberti, M., Begusch, H. & Hearst, J. E. (1984) *Cell* **37,** 949–957.
29. Michel, H., Weyer, K. A., Gruenberg, H., Dunger, I., Oesterhelt, D. & Lottspeich, F. (1986) *EMBO J.* **5,** 1149–1158.
30. Michel, H., Weyer, K. A., Gruenberg, H. & Lottspeich, F. (1985) *EMBO J.* **4,** 1667–1672.